Role of solvation dynamics in the kinetics of solvolysis reactions in microreactors

Pramod Kumar Verma, Abhinanadan Makhal, Rajib Kumar Mitra and Samir Kumar Pal*

Received 19th March 2009, Accepted 4th June 2009
First published as an Advance Article on the web 15th July 2009
DOI: 10.1039/b905573h

In this contribution we attempt to correlate the dynamical states of water molecules in reverse micelles with a solvolysis reaction in accordance with the activation energy barrier crossing model at the micellar interface. Precise measurement of the different dynamical states of water molecules at the reverse micellar interface with various degrees of hydration is achieved through temperature-dependent solvation dynamics of coumarin 523. The rotational anisotropy studies along with a wobbling-in-cone analysis show that the probe residing at the micellar interface pointing towards the core water experiences less microviscosity at elevated temperature. The consequences of the dynamical freedom of the water at elevated temperature in the solvolysis reaction of benzoyl chloride have also been explored. The accelerated rate of solvolysis has been correlated with the increased solvation dynamics, both of which are associated with a temperature-induced transition of bound to free type water molecules at the micellar interface.

Introduction

Reverse micellar (RM) systems have evolved as a potential reaction medium to carry out various chemical reactions otherwise difficult to control in homogeneous media due to highly structured water molecules present in the system.[1–7] In recent years, there have been a number of applications of RMs for controlled enzymatic reaction,[8,9] biomedical informatics,[10] DNA hybridization[11] and its sequence-selective extraction,[12] and size-selective preparation of nanoparticles.[13,14] It is concluded that dynamical freedom of the water molecules present in the RM is responsible for the precise control of the reactions. The two clearly differentiated phases (aqueous and organic) present in the RMs allow compartmentalization of solubilized species at the microscopic level. Different types of surfactants (like non-ionic, anionic, cationic, zwitterionic *etc*.) have been used to formulate RMs, however, the most extensively used surfactant is bis(2-ethylhexyl)-sulfosuccinate (AOT) because it can form spherical RMs in many nonpolar solvents over a wide range of w_0 values (w_0 = [water]/[surfactant] and radius of water pool (r in Å) is empirically defined as $r \approx 2w_0^3$).[15,16] The structures of AOT RMs have been extensively studied using several methods such as ^{1}H NMR,[17,18] IR,[19,20] ESR,[21] photon correlation spectroscopy,[22] SANS,[23,24] dielectric studies,[25] densimetry,[26] calorimetry[27] and molecular dynamics simulations.[28,29] Fluorescence spectroscopy has been used to efficiently determine the viscosity, binding site rigidity and proximity of water in the nano-pool.[30–32] Water present inside the RM can broadly be distinguished as bound type (water molecules hydrogen bonded to the interface) and bulk type. However, a study using FT-IR revealed the existence of four different kinds of water molecules in AOT/isooctane (AOT/i-Oc) RMs, namely, free monomers, dimers at the interface, monomers bonded to the interface, and the bulk type.[33] All these studies reveal that at very low w_0, the water molecules in the pool remain very close and strongly attracted to the polar head groups of the surfactants and hence are rather slow moving. As w_0 increases, the size of the water pool increases, and in such large water pools, the mobility of water molecules becomes relatively high, particularly at the central region of the water pool. This change in mobility of the entrapped water molecules inside the RM has also been reported to affect the reaction kinetics occurring in the RM.[34,35]

Dynamical measurements have been used to characterize the intramicellar water in RMs by various research groups.[36–43] Haseawa *et al*.[44] have measured the microviscosity inside RMs of varying size using a viscosity sensitive probe. For $w_0 < 10$, the water inside RMs has a higher microviscosity than that of bulk water due to the presence of a large fraction of water bound to AOT polar head groups. For RMs with $w_0 > 10$, the viscosity decreases slowly as the size of RMs increases. Solvent reorganization with fluorescent probes in RMs[45,46] reveals two different solvation rates inside the RMs and these time scales are attributed to water bound to the polar head groups of AOT and bulk-like water. While ordinary water molecules relax in the subpicosecond time scale,[47] the solvation dynamics of interfacial water molecules are several times slower and occur in the nanosecond time scale.[41,48] These slow solvation dynamics play an important role in many natural biological processes *e.g*. electron transfer, ion transport, molecular recognition in hydrophilic cavities of proteins and membrane lipid bilayers.[49,50] The origin of the

Unit for Nano Science & Technology, Department of Chemical, Biological & Macromolecular Sciences, S. N. Bose National Center for Basic Sciences, Block JD, Sector III, Salt Lake, Kolkata 700098, India. E-mail: skpal@bose.res.in

slow component is associated with a dynamical equilibrium between bound and free types of water molecules[51] and this equilibrium is extremely sensitive to the external environments such as pressure, temperature *etc*. The transition of bound water to free type at the micellar interface with temperature is governed by an Arrhenius type of activation energy barrier crossing model.[51–53]

Despite the large number of attempts made to study the structure and dynamics of water inside RMs and their effect on ordinary chemical reactions and enzymatic activities, no such attempts have been made to show the reflection of bound to free water transition directly on a chemical reaction occurring inside RMs. Our group has recently initiated a series of studies to investigate the dynamics of water in a micro-heterogeneous system (micelle and RM) as a function of temperature. For these systems, the bound to free water transition has been observed to follow an Arrhenius type barrier crossing model.[40,53–55] In a recent paper, we have shown that the modulation of water dynamics at the RM interface by mixing of surfactants also changes the reaction kinetics at the interface.[56] It is therefore interesting to investigate how a temperature-induced modification of the dynamics of interfacial water affects the reaction kinetics at the RM interface. In the present study, we have explored the picosecond-resolved solvation dynamics of the probe coumarin 523 (C-523) in AOT/i-Oc RMs with varying degrees of hydration (w_0 = 5, 10 and 20) at different temperatures (278, 288, 298, 308 and 328 K) within the structural integrity of the RMs as evidenced from earlier dynamic light scattering (DLS) studies.[40] The choice of w_0 values is justified by the fact that AOT/i-Oc RMs form a well defined water pool at w_0 = 10. At a lower hydration level, the water molecules hydrate only the polar head groups of AOT and at $w_0 \geq 10$, the added water goes into the central water pool to increase its size. To explore the geometrical restriction of the probe, rotational relaxation dynamics of the dye in different RM systems at different temperatures has also been determined by using picosecond-resolved anisotropy decay. To correlate the dynamics of water with its reactivity, we have measured the solvolysis kinetics of benzoyl chloride (BzCl) in the RM nano-environment at different w_0 values and temperatures.

Materials and methods

Sodium bis(2-ethylhexyl)sulfosuccinate (AOT) and isooctane (i-Oc) were purchased from Sigma-Aldrich and used as received. Benzoyl chloride (BzCl) was purchased from Merck. Coumarin 523 (C-523) (Scheme 1) was a product of Exciton.

Coumarin 523

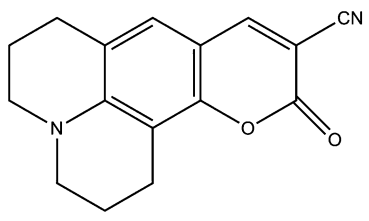

Scheme 1 Molecular structure of coumarin 523.

The RM solutions of C-523 were prepared by adding requisite volumes of aqueous solution of C-523 into a given volume of 100 mM AOT solution in isooctane with vigorous stirring to achieve RMs with the required degree of hydration, w_0. Steady-state absorption and emission were measured with a Shimadzu UV-2450 spectrophotometer and a Jobin Yvon Fluoromax-3 fluorimeter, respectively with a temperature-controlled attachment from Julabo (Model: F32). Fluorescence transients were measured and fitted by using a commercially available spectrophotometer (LifeSpec-ps) from Edinburgh Instruments, UK (excitation wavelength 445 nm (for C-523 in RM systems) and 409 nm (for C-523 in i-Oc), 80 ps instrument response function (IRF)). The details of time-resolved measurements can be found elsewhere.[53] The time-dependent fluorescence Stokes shifts, as estimated from TRES (time-resolved emission spectroscopy), were used to construct the normalized spectral shift correlation function or the solvent correlation function, $C(t)$, defined as

$$C(t) = \frac{\nu(t) - \nu(\infty)}{\nu(0) - \nu(\infty)}, \quad (1)$$

where $\nu(0)$, $\nu(t)$ and $\nu(\infty)$ are the emission maxima (in cm^{-1}) at time zero, t and infinity, respectively. The $C(t)$ function represents the temporal response of the solvent relaxation process, as occurs around the probe following its photo excitation and the associated change in the dipole moment. For anisotropy ($r(t)$) measurements, emission polarization is adjusted to be parallel or perpendicular to that of the excitation, and anisotropy is defined as

$$r(t) = \frac{I_{para} - GI_{perp}}{I_{para} + 2GI_{perp}}. \quad (2)$$

G, the grating factor, was determined following the long time tail matching technique.[57] All the anisotropies were measured at the emission maxima. For the kinetics study of BzCl hydrolysis, a known volume of BzCl in i-Oc was added to 1 ml 100 mM AOT RM such that the overall concentration of BzCl remains 100 μM. The kinetics of solvolysis of BzCl was monitored by time dependent change in the absorbance of BzCl at 288 nm.

Results and discussion

Our main focus of the present study is to correlate the reaction kinetics inside an RM with the solvation dynamics as a function of temperature. As a first step towards this, we investigate the steady-state photophysics of the probe. Fig. 1a shows the absorption spectra of C-523 in i-Oc, water and RMs of w_0 = 5, 10, and 20. The absorption peaks of C-523 in i-Oc and bulk water are obtained at 425 and 455 nm, respectively. On addition of water to the AOT/i-Oc solution, the absorption spectrum shows a shoulder at around 440 nm. The inset of Fig. 1a shows the difference absorption spectra of C-523 in AOT/i-Oc RM at different w_0 values at 298 K, in which the absorption spectrum of C-523 in i-Oc has been subtracted from that of C-523 in AOT/i-Oc RM. It is evident from the figure that a single absorption peak around ~440 nm, which is close to that of the probe in bulk water, is obtained for all the three RM systems. This fact supports the choice of

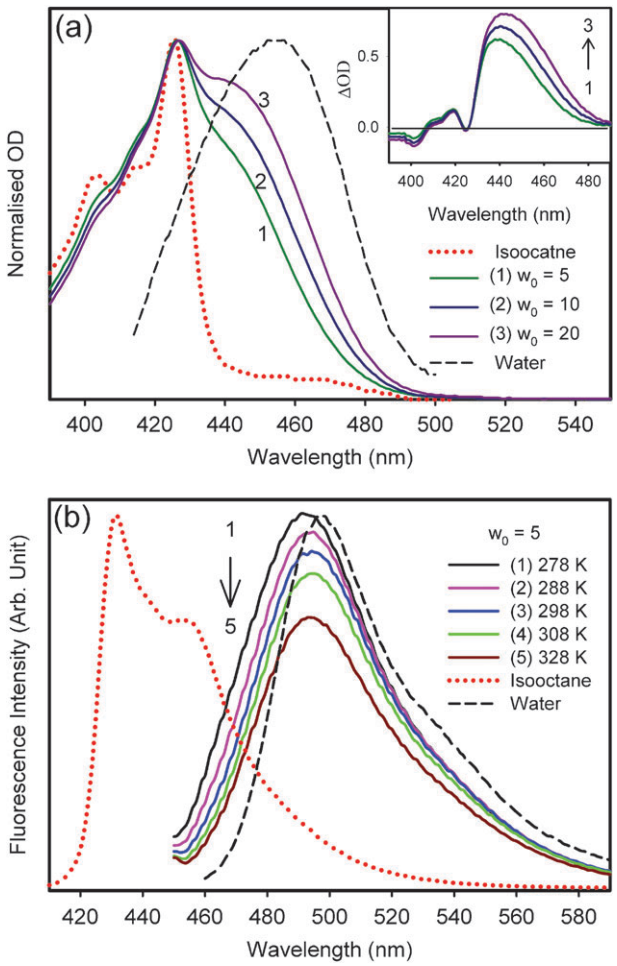

Fig. 1 (a) Absorption spectra of C-523 in i-Oc, water and reverse micelles with w_0 = 5, 10, and 20. Difference absorption spectra of C-523 in AOT/i-Oc RMs (with respect to C-523 in i-Oc) with w_0 = 5, 10 and 20 at 298 K is presented in the inset. (b) Emission spectra of C-523 in i-Oc (λ_{ex} = 409 nm), water (λ_{ex} = 445 nm) and AOT/i-Oc reverse micelles with w_0 = 5 at different temperatures (λ_{ex} = 445 nm).

445 nm wavelength as the excitation source for the time-resolved studies as one would expect information coming only from the aqueous phase or the interphase. The temperature-dependent steady-state fluorescence spectra of C-523 in AOT/i-Oc RM excited at 445 nm at different w_0 values and different temperatures have been measured and one such representative illustration for w_0 = 5 at 278, 288, 298, 308 and 328 K is presented in Fig. 1b. The corresponding emission peaks (λ_{max}) of the emission spectra are presented in Table 1. The fluorescence maximum of C-523 in water is at 498 nm; and that in w_0 = 5, 10, and 20 systems are at 494, 496, and 496 nm, respectively at 298 K. For w_0 = 5, a ~3 nm red shift is observed when the temperature is increased from 278 to 328 K (Table 1). For w_0 = 10 and 20 systems, the emission spectra remain practically unchanged with increase in temperature. A progressive red shift of the fluorescence peak with increasing w_0 is observed (Table 1) which indicates the location of the probe to be at the RM interface pointing towards the core water and signifies that the probe senses a more polar environment at higher hydration level. Wong *et al.*[58,59] concluded that for AOT/i-Oc RM the polarity of the water pool increases as the RM radius increases (dielectric constant values of the interface change from ε = 31 (for w_0 = 1) to ε = 47 (for w_0 = 45.2)). They attributed this increased polarity to an increase in the number of bulk type water molecules in the RM interior. In addition, the micropolarity experiments of Correa *et al.*[60] reveal an increase in the polarity of RM-entrapped water up to w_0 = 10 to reach a plateau. The observed slight (~3 nm) red shift for w_0 = 5 system on increasing the temperature indicates that the probe senses a more polar environment at elevated temperatures. This is due to the fact that the interfacial bound water molecules hydrating the polar head groups become labile upon increase in temperature. The peak shift is negligible for w_0 = 10 and 20 RMs (Table 1).

Let us now concentrate on the dynamics of the water molecules inside the RMs. In i-Oc, the fluorescence decays of C-523 are found to be independent of emission wavelengths, the lifetime being 2.6 ns (λ_{ex} = 409 nm). This indicates that C-523 exhibits no time dependent Stokes shift in i-Oc. Fig. 2a shows the fluorescence transients of C-523 in the w_0 = 10 RM system at 278 and 328 K at three selected wavelengths of 460, 500 and 600 nm. The transient at 460 nm can be fitted tri-exponentially with time components of 0.14 ns (36%), 0.75 ns (47%) and 3.9 ns (17%). For the extreme red wavelength (600 nm), a distinct rise component of 0.58 ns is obtained along with a decay component of 4.2 ns. The presence of faster decay components at the blue end and a rise component at the red wavelength is consistent with the picture of solvation in RM. As the temperature is increased to 328 K, the transients still show wavelength dependency with a decrease in the time constants. Such faster decay transients with increasing temperature indicates the increased mobility of the solvating species at elevated temperatures. A similar trend is also observed at different temperatures for RMs with w_0 = 5 and 20. With increase in w_0, the transients at a particular wavelength and temperature become faster. This observation is attributed to the increased solvent mobility as the micellar interior expands, leaving proportionately less water bound to the micellar interface.

Using the decay transients at different wavelengths, we construct TRES for different w_0 values at different temperatures. A representative TRES for C-523 in AOT/i-Oc RM at 298 K with w_0 = 10 is presented in Fig. 2b where a significant dynamic fluorescence Stokes shift of 514 cm^{-1} in 10 ns is observed. Fig. 2c shows one representative $C(t)$ plot of w_0 = 10 at five different temperatures, and the solvation time constants of various RMs at five different temperatures are presented in Table 1. All these curves are well fitted with bi-exponential decay functions. It is evident from Table 1 that one of the solvation time constants is of the order of several hundreds of picoseconds, while the other is of the order of a few nanoseconds. At low water content (w_0 = 5 at 298 K) the decay consists of a slow time constant of 4.0 ns and a fast time constant of 1.0 ns. At high water content (w_0 = 20 at 298 K) the decay of $C(t)$ is still bi-exponential, but distinctly faster and consists of a component of 0.62 ns and another of 0.11 ns. Both the observed time constants (one slow and the other fast) are much slower than the subpicosecond solvation time

Table 1 Solvent correlation data for C-523 in AOT/i-Oc RMs of various w_0 values at different temperatures[a] and activation energy values for w_0 = 5, 10 and 20

Temperature/K	Fluorescence peak/nm	a_1	τ_1/ns	a_2	τ_2/ns	$\langle\tau_s\rangle$/ns	E_{act}/kcal mol^{-1}
w_0 = 5							
278	491	62	1.30	39	4.4	2.52	5.1
288	494	73	1.10	27	4.2	1.94	
298	494	87	1.01	13	4.0	1.39	
308	494	85	0.63	15	3.7	1.09	
328	494	71	0.44	29	1.0	0.60	
w_0 = 10							
278	495	36	0.52	64	2.14	1.55	6.5
288	495	57	0.47	43	1.67	0.99	
298	496	33	0.30	67	0.80	0.63	
308	496	32	0.11	67	0.58	0.42	
328	496	37	0.07	63	0.38	0.26	
w_0 = 20							
278	496	53	0.54	47	2.26	1.35	7.4
288	496	62	0.36	38	1.71	0.87	
298	496	34	0.11	66	0.62	0.45	
308	496	39	0.07	61	0.50	0.33	
328	496	49	0.05	51	0.30	0.18	

[a] τ represents the solvent correlation time constants, a represents its relative percentage.

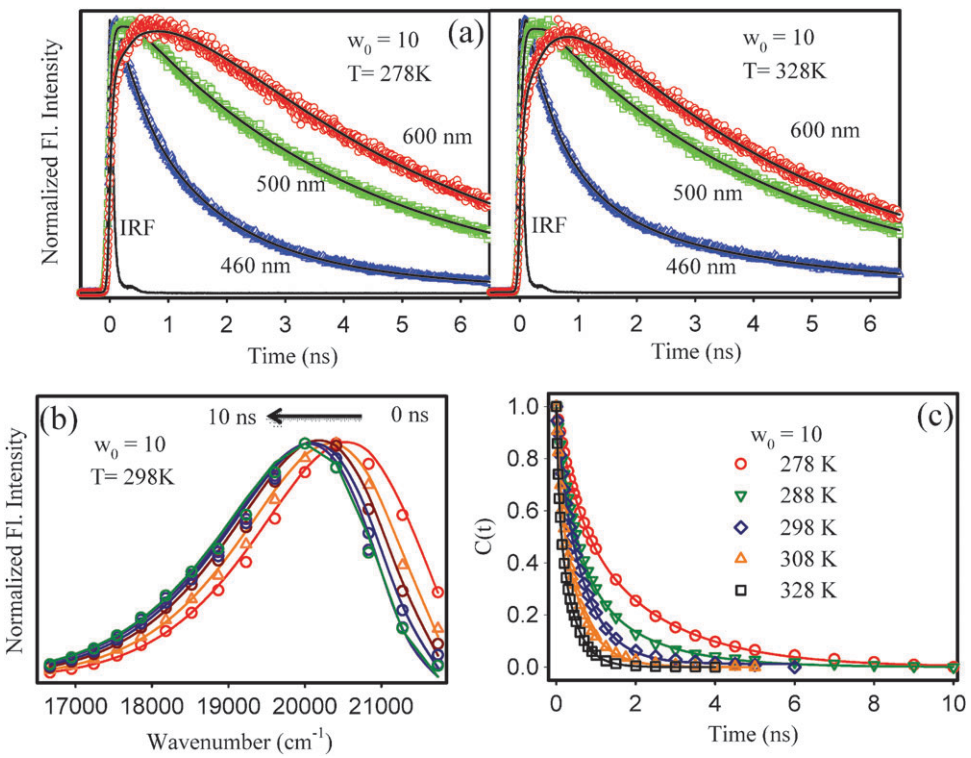

Fig. 2 (a) Fluorescence decay transients of C-523 in AOT/i-Oc reverse micelles with w_0 = 10 at 278 and 328 K. (b) Time-resolved emission spectra (TRES) for w_0 = 10 RM at 298 K. (c) Solvation correlation function, $C(t)$, of C-523 in RM (w_0 = 10) at different temperatures.

constant of bulk water.[47] The observed slow and fast components are attributed to the interfacial bound type and free type water molecules, respectively present in the RM. The time constants are consistent with those reported earlier for RM systems.[40,41,43,61] It is to be noted that, due to our limited instrumental resolution (IRF ~80 ps), an ultrafast component, which is due to the fast moving bulk-like water molecules, is missed in our measurements. But this ultrafast component is mainly attributed to the fast moving bulk type water molecules present in the RM core. Since our focus of the present work is to correlate the kinetics of a reaction occurring at the interface of the RM with the dynamics of water molecules, our discussion would still be meaningful if made on the interfacial slow moving water molecules detectable with our TCSPC setup. The overall decrease of $\langle\tau_s\rangle$ ($\langle\tau_s\rangle = a_1\tau_1 + a_2\tau_2$) on increasing temperature for all the three systems reveals that an increase in temperature accelerates the solvation process at the interface irrespective

of the water pool size. Different experimental evidences indicate that even in a larger water pool ($w_0 \geq 10$), the properties of the confined water differ from those of the bulk water.[62–64] Thus, almost bulk-like behaviour of water inside the pool is not expected even at higher w_0 values. The slow timescales observed in the present systems are due to the slow moving, interfacially bound water molecules that become faster upon an increase in the temperature.

The temperature-induced acceleration of solvation dynamics of water in AOT/i-Oc RM, can be explained with the help of the multishell continuum model proposed by Bagchi *et al.*[51,65–68] for RMs and proteins. In this model, a dynamic exchange between free and bound water molecules is assumed. The energetic of the exchange depends upon the strength and the number of hydrogen bonds among the water molecules at the interface. The bound to free type transition of water molecules with temperature is assumed to be governed by an Arrhenius type of activation energy barrier crossing model.[51–53] We fit an Arrhenius plot using the $\langle\tau_s\rangle$ values listed in Table 1 for all the three systems (Fig. 3). Plots of ln $(1/\langle\tau_s\rangle)$ *vs.* $1/T$ produce good linear fits with corresponding activation energy values of 5.1 ± 0.5, 6.5 ± 0.6, and 7.4 ± 0.7 kcal mol^{-1} for w_0 = 5, 10 and 20 RMs, respectively (Table 1). The E_{act} value of 5.1 kcal mol^{-1} for w_0 = 5 system is of the order of 2.4–4 kcal mol^{-1}, the energy barrier calculated for the transition from bound type water (hydrogen bonded to polar head group of RM, denoted as IBW, Scheme 2) to free type water (not directly hydrogen bonded to head group, denoted as IFW, Scheme 2) at the RM and micellar interface.[53,69] In a previous study, we obtained an E_{act} value of 3.4 kcal mol^{-1} using a C-500 probe[40] for the same system. It is to be noted that C-500 is sparingly soluble in water and therefore resides mainly at the RM interface, and thus can precisely report the E_{act} value corresponding to the transition occurring at the RM interface. C-523, on the other hand, has considerable water solubility and thus the E_{act} value obtained at w_0 = 5 is higher than that expected (2.4–4 kcal mol^{-1}). For the hydrated systems ($w_0 \geq 10$), wherein the RM water pool is formed, the probe senses a transition from bound to free or bulk type water molecules (water molecules in the core of the RMs, denoted as FW, Scheme 2) which is associated with a higher energy barrier (7–8 kcal mol^{-1})[52] and the E_{act} values obtained in the present study (6.5 and 7.4 kcal mol^{-1}) are in an excellent agreement with that. E_{act} values are comparable for w_0 = 10 and 20 systems, as in both of these systems, the probe experiences a bound to bulk type transition, with the latter system richer in the bulk type water molecules.

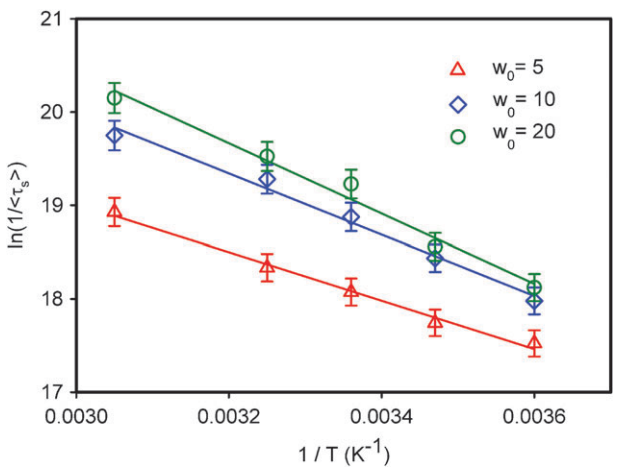

Fig. 3 Plot of ln $(1/\langle\tau_s\rangle)$ against $1/T$ for AOT/i-Oc RM with w_0 = 5, 10 and 20, with linear fits.

To have a further idea of the temperature-mediated modification of interfacial water dynamics, we measure the temporal anisotropy decay, $r(t)$, of the probe in AOT/i-Oc RMs at different w_0 values and temperatures. A representative diagram for the w_0 = 10 system at 278 and 328 K is given in Fig. 4a. The rotational correlation time constants for all the systems are given in Table 2. The time constants obtained for the w_0 = 10 systems at 298 K are in good agreement with those reported by Mitra *et al.*[40] and Majumdar *et al.*[39] It is found that the slower time constant decreases with increasing w_0 and temperature for all the studied systems, similar to that reported earlier,[40,61] indicating that the probe is more free to move in larger RMs and at higher temperatures. To account for the effect of temperature on the rotational relaxation process of the probe inside the RM, the bi-exponential anisotropy decay is analyzed using the two-step wobbling-in-cone model.[70–73] Assuming that the slow and fast motions are separable, the slow (τ_{slow}) and fast (τ_{fast}) rotational time constants can be related as

$$\frac{1}{\tau_{slow}} = \frac{1}{\tau_l} + \frac{1}{\tau_m}, \qquad \frac{1}{\tau_{fast}} = \frac{1}{\tau_w} + \frac{1}{\tau_{slow}}, \tag{3}$$

where, τ_l and τ_w are the time constants for the lateral diffusion and the wobbling motion of the probe, respectively. The time constant for the overall rotation of the RM, τ_m, is given by the Stokes–Einstein–Debye equation:

$$\tau_m = \frac{\eta V_h}{k_B T}, \tag{4}$$

where, V_h is the hydrodynamic volume of the RM and η is the viscosity of the dispersing solvent. Note that τ_m values are an order of the magnitude higher than the τ_{fast} and τ_{slow} values and, thus, the overall rotation of the RM does not contribute to the decay of the anisotropy. In view of this, τ_{fast} and τ_{slow} essentially represent the time constants for wobbling motion and lateral diffusion, respectively.

According to this model, the rotational anisotropy decay function is denoted as

$$r(t) = r_0[\beta\, e^{-t/\tau_{slow}} + (1 - \beta)\, e^{-t/\tau_{fast}}] \tag{5}$$

where $\beta = S^2$, and S is the generalized order parameter that describes the degree of restriction on the wobbling-in-cone orientational motion. Its magnitude is considered as a measure of the spatial restriction of the probe and can have a value from zero (for unrestricted rotation of the probe) to one (for completely restricted motion). The semicone angle, θ_w is related to the ordered parameter as

$$S = \tfrac{1}{2}\cos\theta_w\,(1 + \cos\theta_w). \tag{6}$$

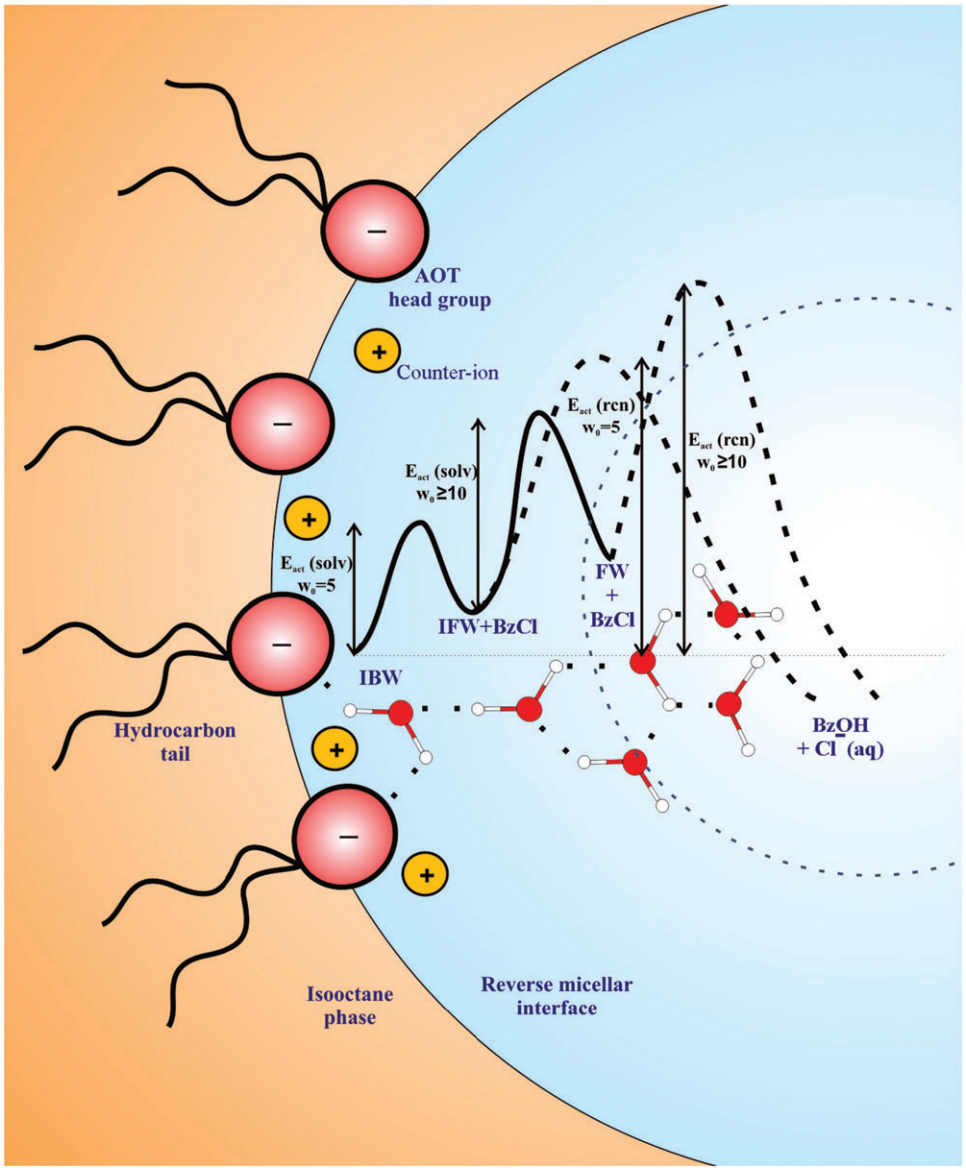

Scheme 2 Correlation between the dynamics and reactivity of water at the AOT–isooctane reverse micellar interface. IBW, IFW and FW stand for interfacially bound water, interfacial free water and free water, respectively. E_{act}(solv) and E_{act}(rcn) denotes the activation energies calculated from temperature dependent solvation dynamics studies (Table 1) and reaction kinetics studies (Table 3). Note that benzoyl chloride (BzCl) reacts with either IFW or FW at the micellar interface to produce benzoyl hydroxide (BzOH).

The diffusion coefficient for wobbling motion, D_w, can be obtained from the following equation

$$D_w = \frac{1}{(1-S^2)\tau_w}\left[\frac{x^2(1+x)^2}{2(x-1)}\left\{\ln\left(\frac{1+x}{2}\right)+\frac{1-x}{2}\right\} + \frac{1-x}{24}(6+8x-x^2-12x^3-7x^4)\right], \quad (7)$$

where $x = \cos\theta_w$. The results obtained from the analysis are summarized in Table 2 and Fig. 4b. As evidenced from Table 2, the wobbling cone angle (θ_w), which is the semicone inscribed by C-523 at the RM interface, increases with increase in temperature for all the w_0 (= 5, 10 and 20) values. The diffusion coefficient (D_w) values are of the same order of magnitude as reported earlier for RM systems[40,61] and increases with increasing temperature for all the w_0 values. The increase in θ_w and D_w implies that with increasing temperature, the probe experiences less restricted rotation at the RM interface which might be due to the faster movement of the trapped water at elevated temperatures and/or diffusion of the probe toward the central bulk type water of the RMs. Such an increase in D_w is associated with a decrease in the microviscosity at the RM interface[51,74,75] which corroborates the conversion of surface bound water to free water.[51,69,76] This change causes the observed faster solvation dynamics at elevated temperatures. Note that the θ_w and D_w values are comparable in w_0 = 10 and 20 systems at all temperatures. Thus, the probe experiences a similar type of micro-environment in these two systems and is in agreement with the steady-state and solvation dynamics results.

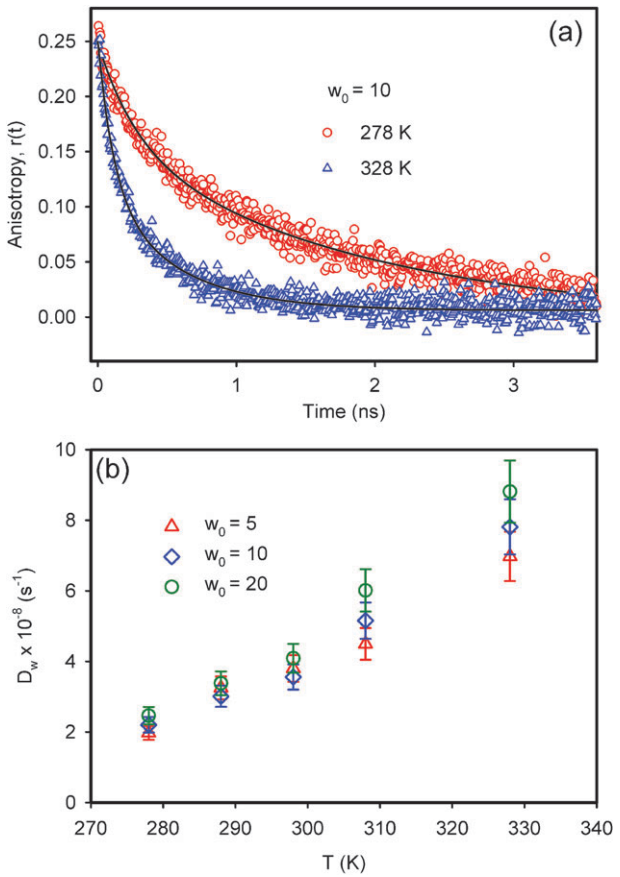

Fig. 4 Time-resolved anisotropy decay, $r(t)$, of C-523 in AOT/i-Oc RMs of w_0 = 10 at 278 and 328 K. (b) Diffusion coefficient for wobbling-in-cone motion (D_w) of C-523 in RMs at different temperatures.

Table 2 Fluorescence anisotropy decay and wobbling-in-cone data of C-523 in AOT/i-Oc RMs at different w_0 and temperature values (r_0 defines anisotropy at time t = 0)

Temperature/K	r_0	a_{fast}	τ_{fast}/ns	a_{slow}	τ_{slow}/ns	θ_w/°	$D_w \times 10^{-8}$/s^{-1}
w_0 = 5							
278	0.29	0.32	0.29	0.68	1.99	28.6	2.0
288	0.31	0.41	0.23	0.59	1.60	33.1	3.2
298	0.29	0.43	0.20	0.57	1.18	34.0	3.8
308	0.27	0.46	0.18	0.54	0.93	35.9	4.5
328	0.26	0.52	0.13	0.48	0.63	38.7	7.0
w_0 = 10							
278	0.29	0.36	0.29	0.64	1.80	30.7	2.2
288	0.29	0.44	0.26	0.56	1.40	35.0	3.0
298	0.27	0.46	0.22	0.54	1.00	35.8	3.6
308	0.25	0.48	0.16	0.52	0.80	36.7	5.2
328	0.25	0.54	0.12	0.46	0.54	40.0	7.8
w_0 = 20							
278	0.30	0.35	0.25	0.65	1.60	30.0	2.5
288	0.28	0.44	0.23	0.56	1.20	35.0	3.4
298	0.28	0.50	0.21	0.5	0.96	37.8	4.1
308	0.28	0.58	0.17	0.42	0.80	41.8	6.0
328	0.22	0.71	0.15	0.29	0.70	49.6	8.8

Knowing about the temperature-activated modification of the water dynamics at the RM interface we now focus on the kinetics of the solvolysis reaction at the RM interface. In order to investigate whether the transition of surface-bound to free type water molecules inside the RMs has any effect on the activation energy of a reaction taking place inside the RM, we measure the kinetics of a well studied[34,35,77–79] solvolysis reaction of benzoyl chloride (BzCl) in w_0 = 5, 10 and 20 RMs at 288, 298, 308, 328 and 348 K. BzCl is solubilized in i-Oc and then added into the RM, wherein it gets compartmentalized into the organic phase and the interphase. According to the pseudo-phase model proposed by Garcia-Rio *et al.*,[34,77–79] assuming a zero solubility of BzCl in the aqueous phase, the reaction rate can be written in the form, rate = k_i [BzCl], where [BzCl] is the concentration of BzCl at the interface and k_i is the intrinsic rate constant given as $k_i = k_{obs}(1 + Z/K_{oi})$, where Z is the ratio of molar concentration of i-Oc and AOT, which has been kept constant throughout our study, k_{obs} is the observed rate constant, and K_{oi} is the distribution constant for the BzCl distribution between the oil phase and the interface. Determination of K_{oi} needs a detailed study of k_{obs} at different Z. However, previous studies[35] show that for the AOT/i-Oc system, K_{oi} for BzCl does not change appreciably (K_{oi} is 2.5 at w_0 = 5, and varies between 4.0 to 4.2 for w_0 = 6 to 50). Also K_{oi} changes only marginally with temperature for different substituted benzoyl chlorides,[78] and the K_{oi} values are comparable for AOT and non-ionic Brij-30 RM systems.[80] So, for a first approximation, we can assume k_{obs} does not depend on K_{oi} and made our further discussion on the light that the reaction follows a first order kinetics with a rate constant of k_{obs}.

The reaction is monitored by measuring the time-dependent decrease in the absorbance of BzCl at 288 nm. Fig. 5a shows representative decay kinetics of BzCl at w_0 = 10 at different temperatures. k_{obs} of the hydrolysis reaction in different sized RMs at different temperatures are given in Table 3. It is important to point out that the values of k_{obs} for higher w_0, as well as for smaller w_0, are smaller than the value observed in bulk water (k = 1.1 s^{-1})[80] indicating that the reaction is occurring at the interface of the RM. It is observed that the rate of hydrolysis of BzCl increases with increase in w_0 at a particular temperature (Table 3). It has been reported earlier[34,35] that this increase has its origin in the increase in the fraction of interfacial free type water molecules and, hence, the increase in the possibility to solvate the leaving group (here Cl^-) inside the RM. Thus, the faster dynamics of the water molecules as evidenced from the solvation study are also manifested here in the form of faster kinetics. The overall decrease of k_{obs} with increase in temperature for all the three w_0 values indicates that an increase in temperature accelerates the nucleuophilic reaction at the interface. From the previous studies of Garcia-Rio *et al.*,[35] it can be noticed that the rate constant of the solvolysis of BzCl in AOT/i-Oc RM does not change appreciably up to $w_0 < 10$, and then increases steadily with increase in w_0. It could be recalled here that the contribution of IFW is negligible in the $w_0 < 10$ region, and starts increasing beyond $w_0 \geq 10$, only after the hydration of the AOT headgroup is complete and a well-defined water pool is formed inside the RM. This correlation confirms the fact that the free type interfacial water molecules act as the nucleophile in the solvolysis reaction. The observed acceleration of k_{obs} with temperature (Table 3) is due to the acceleration of the slow moving interfacial water molecules at elevated temperature as has been observed in the present solvation

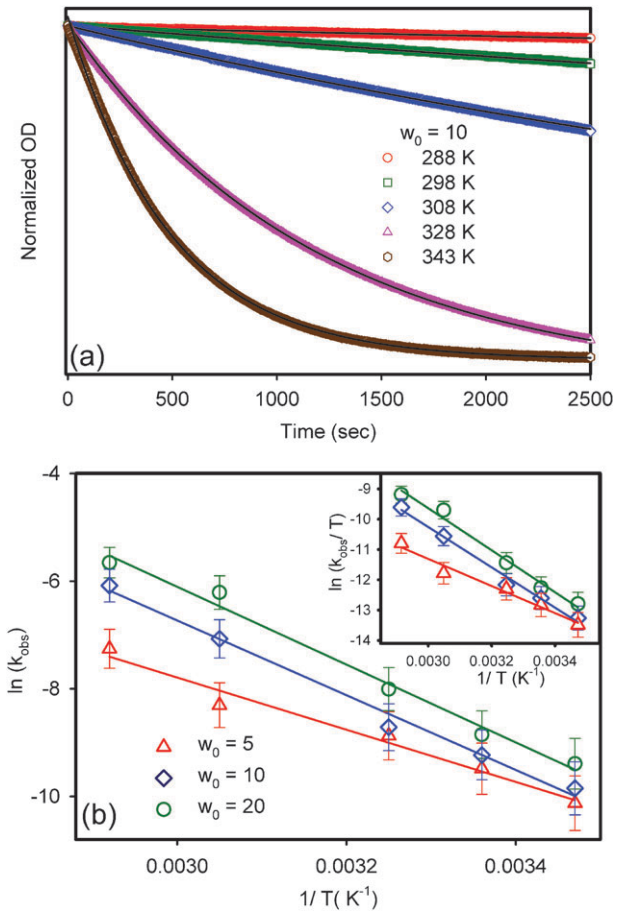

Fig. 5 (a) Decay kinetics of solvolysis of benzoyl chloride monitored at 288 nm for w_0 = 20 RMs at different temperatures. (b) Arrhenius (ln (k_{obs}) *vs.* $1/T$) plot for solvolysis of benzoyl chloride inside RMs, w_0 = 5, 10 and 20. The Eyring plots for the same systems are shown in the inset.

dynamics study. At low temperature, most of the interfacial water molecules are involved in the solvation of the anionic head group and therefore are not available to assist nucleophilic attack at the acyl carbon. With increase in temperature, the fraction of free water in the RM interphase increases and hence also the kinetics become faster. In order to determine the dependency of the rate of the reaction on temperature, we apply the Arrhenius model and plotted ln (k_{obs}) against $1/T$ for all the RMs (Fig. 5b). Good linear fits in all the RMs are obtained with E_{act} values of 9.8 ± 1.0, 13.7 ± 1.4 and 14.3 ± 1.4 kcal mol^{-1} for w_0 = 5, 10 and 20, respectively. Note that the E_{act} values obtained from the kinetic measurements (E_{act}(rcn)) are higher than those obtained from the solvation measurements (E_{act}(solv)). Also, the E_{act}(rcn) values are comparable for w_0 = 10 and 20 systems, a fact corroborating our present solvation dynamics studies, wherein comparable E_{act}(solv) values are obtained for w_0 = 10 and 20 systems. To establish the dependency of reaction kinetics with w_0, we determine the values of $\Delta H^{\neq}$ and $\Delta S^{\neq}$ by fitting the k_{obs} data in an Eyring equation,

$$\ln\left(\frac{k_{obs}}{T}\right) = \ln\left(\frac{k_B}{h}\right) + \frac{\Delta S^{\neq}}{R} - \frac{\Delta H^{\neq}}{RT}, \qquad (8)$$

where k_B and h are Boltzmann and Plank constants, respectively, $\Delta S^{\neq}$ and $\Delta H^{\neq}$ are the activation parameters. We plot ln (k_{obs}/T) against $1/T$ and all the three systems produce good linear fits (Fig. 5b, inset) and the corresponding $\Delta H^{\neq}$ values obtained are 8.9, 13.2 and 13.7 kcal mol^{-1} for w_0 = 5, 10 and 20 systems, respectively. These values are in close agreement with those obtained by Fernandez *et al.*[78] for different substituted benzoyl chlorides. Fernandez *et al.*,[78] however, used k_i, whereas we have used k_{obs} in the Eyring equation, and the proximity of the obtained $\Delta H^{\neq}$ values supports our assumption of considering K_{oi} to be a constant for all the systems and the solvolysis reaction to follow a pseudo first order kinetics. The $\Delta S^{\neq}$ values are obtained to be −34, −19 and −16 cal K^{-1} mol^{-1} for w_0 = 5, 10 and 20 systems respectively, which are also in the same order of magnitude as obtained by Fernandez *et al.*[78] The gradual increase in the $\Delta S^{\neq}$ values indicates the ease of the reaction with increasing w_0, as has also been observed from the k_{obs} values (Table 3).

The solvolysis process in the RM systems could be assumed to be divided into two steps (Scheme 2); as an initial step, free water molecules are formed at the RM interface. This process is dependent on w_0 and the corresponding E_{act}(solv) values are of ~3–4 kcal mol^{-1} for the less hydrated system (w_0 = 5) and ~6–8 kcal mol^{-1} for hydrated systems (w_0 = 10 and 20). As a following step, these free water molecules act as nucleophiles to bring about the solvolysis process. This process is supposed to be independent of the hydration of RM. If we take the difference of E_{act}(solv) and E_{act}(rcn), an almost constant value of ΔE_{act} (~7 kcal mol^{-1}), a value responsible for the formation of the solvolysis product and supposed to be irrespective of the level of hydration in RM, is obtained for the w_0 = 10 and 20 systems. However, for the w_0 = 5 system, the observed difference is rather low (4.6 kcal mol^{-1}). It is to be noted here that the E_{act}(solv) obtained for w_0 = 5 in the present study is somewhat larger compared to an E_{act}(solv)

Table 3 Rate constants (observed, k_{obs}) for solvolysis of benzoyl chloride in RMs at different w_0 and temperatures and activation energy values for w_0 = 5, 10 and 20

	w_0 = 5		w_0 = 10		w_0 = 20	
Temperature (K)	$k_{obs} \times 10^4$/s^{-1}	E_{act}/kcal mol^{-1}	$k_{obs} \times 10^4$/s^{-1}	E_{act}/kcal mol^{-1}	$k_{obs} \times 10^4$/s^{-1}	E_{act}/kcal mol^{-1}
288	0.4	9.8	0.5	13.7	0.8	14.3
298	0.8		1.0		1.4	
308	1.4		1.6		3.3	
328	2.5		8.5		20	
343	7.0		23		35	

value of 3.4 kcal mol^{-1} obtained in our previous study[40] using coumarin 500 as the fluorophore for an identical system. For a less hydrated system like $w_0 = 5$, the expected value of E_{act}(solv) should vary between 2.4–4 kcal mol^{-1}, and the higher value obtained in the present study might be due to the considerable solubility of C-523 in water as has been discussed in earlier sections. Considering an ideal E_{act}(solv) value of 3.4 for the $w_0 = 5$ system, the ΔE_{act} value comes out to be 6.4 kcal mol^{-1} which is in good agreement with those obtained for the other RM systems. It could also be noted here that the solvolysis reaction proceeds through a dissociative mechanism for $w_0 \geq 10$ RM systems, whereas for the $w_0 = 5$ RM system, the associative mechanism prevails, which might also account for the observed discrepancy in the ΔE_{act} values at low hydration. The E_{act}(rcn) values obtained experimentally include both E_{act}(solv) and ΔE_{act} values (Scheme 2). The former one is dependent on the w_0 values, whereas the latter one is independent of w_0. The ΔE_{act} value corresponds to the reaction of the free water molecules with BzCl and thus does not depend upon any other factor. It is only the availability of the free interfacial water molecules that governs the E_{act}(rcn) values, which in turn depends upon the E_{act}(solv) values. The difference in E_{act}(rcn) values for $w_0 = 5$ and $w_0 \geq 10$ systems ($\sim$4–5 kcal/mol) is thus found to be in excellent agreement with the difference between the calculated difference of IBW to IFW (2.4–4 kcal/mol) and IBW to FW (7–8 kcal/mol) transition. It is interesting to note that E_{act}(rcn) are comparable for $w_0 = 10$ and 20 systems since their E_{act}(solv) values are also comparable and in both of these systems, a well defined water pool persists. Thus the dynamics of water molecules at the RM interface (depending upon the degree of hydration and temperature) is correlated with the observed reaction kinetics at the interface.

Conclusion

Our report explores the temperature-dependent dynamics of solvation of a probe, C-523, in AOT/i-Oc RM with various degrees of hydration. The observed acceleration of solvation dynamics with temperature supports the general view that the mobility of the water molecules in RM increases with temperature due to the transition of surface bound water to free water at elevated temperature. Assuming an Arrhenius energy barrier crossing model, the E_a is found to be 5 kcal mol^{-1} for $w_0 = 5$, indicating exchange between interfacially bound type water molecules to interfacially free type water molecules. For the hydrated RMs ($w_0 = 10$ and 20, wherein a definite water pool is formed), E_a values are higher, indicating a bound to bulk type transition of water molecules. The rotational anisotropy study also corroborates with this result as the probe experiences less microviscosity at elevated temperatures. Applying the Arrhenius model to the solvolysis of BzCl shows that the differences between activation energy barriers for the solvolysis at different w_0 values are attributed to the formation and availability of free water molecules at the interface, which in turn depends upon w_0. Our present study is expected to find a general application in the control of various reactions in the nano-environment of RM.

Acknowledgements

P.K.V and A.M. thank CSIR for research fellowships. We thank DST for a financial grant (SR/SO/BB-15/2007).

References

1 V. Uskoković and M. Drofenik, *Adv. Colloid Interface Sci.*, 2007, **133**, 23–34.
2 M.-F. Ruasse, I. B. Blagoeva, R. Ciri, L. Garcia-Rio, J. R. Leis, A. Marques, J. Mejuto and E. Monnier, *Pure Appl. Chem.*, 1997, **69**, 1923.
3 M. P. Pileni, *Adv. Colloid Interface Sci.*, 1993, **46**, 139–163.
4 G. Astray, A. Cid, L. García-Río, P. Hervella, J. C. Mejuto and M. Pérez-Lorenzo, *Prog. React. Kinet. Mech.*, 2008, **33**, 81.
5 J. Rodriguez, D. Laria, E. Guàrdia and J. Martí, *Phys. Chem. Chem. Phys.*, 2009, **11**, 1484–1490.
6 N. Gorski and Y. M. Oatanevich, *Ber. Bunsen-Ges. Phys. Chem.*, 1990, **94**, 737.
7 L. K. Shrestha, T. Sato and K. Aramaki, *Phys. Chem. Chem. Phys.*, 2009, in press.
8 A. L. Creagh, J. M. Prausnitz and H. W. Blanch, *Enzyme Microb. Technol.*, 1993, **15**, 383.
9 R. Biswas and S. K. Pal, *Chem. Phys. Lett.*, 2004, **387**, 221–226.
10 F. Despa, *Phys. Chem. Chem. Phys.*, 2008, **10**, 4740–4747.
11 L. C. Park, T. Maruyama and M. Goto, *Analyst*, 2003, **128**, 161–165.
12 T. Maruyama, T. Hosogi and M. Goto, *Chem. Commun.*, 2007, 4450–4452.
13 A. B. Smetana, J. S. Wang, J. Boeckl, G. J. Brown and C. M. Wai, *Langmuir*, 2007, **23**, 10429.
14 Q. Yan, A. Purkayastha, T. Kim, R. Kröger, A. Bose and G. Ramanath, *Adv. Mater.*, 2006, **18**, 2569.
15 T. K. De and A. Maitra, *Adv. Colloid Interface Sci.*, 1995, **59**, 95–193.
16 S. Nave, J. Eastoe, R. K. Heenan, D. Steytler and I. Grillo, *Langmuir*, 2000, **16**, 8741–8748.
17 J. H. Fendler, E. J. Fendler, R. T. Medary and V. A. Woods, *J. Am. Chem. Soc.*, 1972, **94**, 7288–7295.
18 M. L. Stahla, B. Baruah, D. M. James, M. D. Johnson, N. E. Levinger and D. C. Crans, *Langmuir*, 2008, **24**, 6027–6035.
19 I. R. Piletic, D. E. Moilanen, N. E. Levinger and M. D. Fayer, *J. Am. Chem. Soc.*, 2006, **128**, 10366–10367.
20 D. E. Moilanen, N. E. Levinger, D. B. Spry and M. D. Fayer, *J. Am. Chem. Soc.*, 2007, **129**, 14311–14318.
21 M. Hu and L. Kevan, *J. Phys. Chem.*, 1990, **94**, 5348.
22 M. Zulauf and H.-F. Eicke, *J. Phys. Chem.*, 1979, **83**, 480–486.
23 A. M. Howe, C. Toprakcioglu, J. C. Dore and B. H. Robinson, *J. Chem. Soc., Faraday Trans. 1*, 1986, **82**, 2411–2422.
24 N. Gorski and Y. M. Oatanevich, *Journal de Physique IV*, 1993, **03**, 149.
25 M. D. Angelo, D. Fioretto, G. Onori, L. Palmieri and A. Santucci, *Phys. Rev. E*, 1996, **54**, 993–996.
26 Y. Yoshimura, I. Abe, M. Ueda, K. Kajiwara, T. Hori and Z. A. Schelly, *Langmuir*, 2000, **16**, 3633–3635.
27 X. Shen, H. Gao and X. Wang, *Phys. Chem. Chem. Phys.*, 1999, **1**, 463–469.
28 J. Faeder and B. M. Ladanyi, *J. Phys. Chem. B*, 2005, **109**, 6732–6740.
29 J. Faeder and B. M. Ladanyi, *J. Phys. Chem. B*, 2000, **104**, 1033–1046.
30 E. M. Corbeil, R. E. Riter and N. E. Levinger, *J. Phys. Chem. B*, 2004, **108**, 10777–10784.
31 N. M. Correa and N. E. Levinger, *J. Phys. Chem. B*, 2006, **110**, 13050–13061.
32 K. Bhattacharyya, *Acc. Chem. Res.*, 2003, **36**, 95–101.
33 C. González-Blanco, L. J. Rodríguez and M. M. Velázquez, *J. Colloid Interface Sci.*, 1999, **211**, 380.
34 L. Garcia-Rio, J. R. Leis and J. A. Moreira, *J. Am. Chem. Soc.*, 2000, **122**, 10325–10334.
35 L. Garcia-Rio, J. R. Leis and E. Iglesias, *J. Phys. Chem.*, 1995, **99**, 12318–12326.
36 D. Pant and N. E. Levinger, *Langmuir*, 2000, **16**, 10123–10130.
37 D. Pant, R. E. Riter and N. E. Levinger, *J. Chem. Phys.*, 1998, **109**, 9995–10003.
38 N. E. Levinger, *Curr. Opin. Colloid Interface Sci.*, 2000, **5**, 118.

39 P. Majumder, R. Sarkar, A. K. Shaw, A. Chakraborty and S. K. Pal, *J. Colloid Interface Sci.*, 2005, **290**, 462.
40 R. K. Mitra, S. S. Sinha and S. K. Pal, *Langmuir*, 2008, **24**, 49–56.
41 N. Sarkar, K. Das, A. Datta, S. Das and K. Bhattacharyya, *J. Phys. Chem.*, 1996, **100**, 10523–10527.
42 P. Dutta, P. Sen, S. Mukherjee, A. Halder and K. Bhattacharyya, *J. Phys. Chem. B*, 2003, **107**, 10815–10822.
43 P. Hazra and N. Sarkar, *Chem. Phys. Lett.*, 2001, **342**, 303–311.
44 M. Hasegawa, T. Sugimura, Y. Shindo and A. Kitahara, *Colloids Surf., A*, 1996, **109**, 305.
45 J. Zhang and F. V. Bright, *J. Phys. Chem.*, 1991, **95**, 7900–7907.
46 C. H. Cho, M. Chung, J. Lee, T. Nguyen, S. Singh, M. Vedamuthu, S. Yao, J.-B. Zhu and G. W. Robinson, *J. Phys. Chem.*, 1995, **99**, 7806–7812.
47 R. Jimenez, G. R. Fleming, P. V. Kumar and M. Maroncelli, *Nature*, 1994, **369**, 471–473.
48 S. Das, A. Datta and K. Bhattacharyya, *J. Phys. Chem. A*, 1997, **101**, 3299–3304.
49 M. Marchi, F. Sterpone and M. Ceccarelli, *J. Am. Chem. Soc.*, 2002, **124**, 6787–6791.
50 M. M. Teeter, A. Yamano, B. Stec and U. Mohanty, *Proc. Natl. Acad. Sci. U. S. A.*, 2001, **98**, 11242.
51 N. Nandi and B. Bagchi, *J. Phys. Chem. B*, 1997, **101**, 10954–10961.
52 S. Sen, S. Mukherjee, A. Halder and K. Bhattacharyya, *Chem. Phys. Lett.*, 2004, **385**, 357–361.
53 R. K. Mitra, S. S. Sinha and S. K. Pal, *J. Phys. Chem. B*, 2007, **111**, 7577–7581.
54 D. Banerjee, S. S. Sinha and S. K. Pal, *J. Phys. Chem. B*, 2007, **111**, 14239.
55 S. S. Narayanan, S. S. Sinha, R. Sarkar and S. K. Pal, *J. Phys. Chem. B*, 2008, **112**, 2859.
56 R. K. Mitra, S. S. Sinha, P. K. Verma and S. K. Pal, *J. Phys. Chem. B*, 2008, **112**, 12946–12953.
57 D. V. O'Connor and D. Philips, *Time Correlated Single Photon Counting*, Academic Press, London, 1984.
58 M. Wong, J. K. Thomas and M. Graetzel, *J. Am. Chem. Soc.*, 1976, **98**, 2391–2397.
59 M. Wong, J. K. Thomas and T. Nowak, *J. Am. Chem. Soc.*, 1977, **99**, 4730–4736.
60 N. M. Correa, M. A. Biasutti and J. J. Silber, *J. Colloid Interface Sci.*, 1995, **172**, 71.
61 A. K. Shaw and S. K. Pal, *J. Phys. Chem. B*, 2007, **111**, 4189–4199.
62 A. Amararene, M. Gindre, J.-Y. Le Huerou, C. Nicot, W. Urbach and M. Waks, *J. Phys. Chem. B*, 1997, **101**, 10751–10756.
63 M. D'Angelo, D. Fioretto, G. Onori, L. Palmieri and A. Santucci, *Phys. Rev. E*, 1996, **54**, 993–996.
64 G. Carlstroem and B. Halle, *Langmuir*, 1988, **4**, 1346–1352.
65 N. Nandi, K. Bhattacharyya and B. Bagchi, *Chem. Rev.*, 2000, **100**, 2013–2045.
66 K. Bhattacharyya and B. Bagchi, *J. Phys. Chem. A*, 2000, **104**, 10603–10613.
67 N. Nandi and B. Bagchi, *J. Phys. Chem. A*, 1998, **102**, 8217–8221.
68 R. Biswas and B. Bagchi, *J. Phys. Chem. A*, 1999, **103**, 2495–2500.
69 S. Pal, S. Balasubramaian and B. Bagchi, *J. Phys. Chem. B*, 2003, **107**, 5194–5202.
70 G. Lipari and A. Szabo, *J. Chem. Phys.*, 1981, **75**, 2971–2976.
71 G. Lipari and A. Szabo, *J. Am. Chem. Soc.*, 1982, **104**, 4546–4559.
72 G. Lipari and A. Szabo, *Biophys. J.*, 1980, **30**, 489.
73 C. C. Wang and R. Pecora, *J. Chem. Phys.*, 1980, **72**, 5333–5340.
74 G. B. Dutt, *J. Phys. Chem. B*, 2003, **107**, 10546–10551.
75 G. B. Dutt, *J. Phys. Chem. B*, 2005, **109**, 4923–4928.
76 S. Pal, S. Balasubramaian and B. Bagchi, *J. Chem. Phys.*, 2002, **117**, 2852–2859.
77 L. Garcia-Rio, J. R. Leis and J. C. Mejuto, *Langmuir*, 2003, **19**, 3190–3197.
78 E. Fernández, L. García-Río, A. Godoy and J. R. Leis, *New J. Chem.*, 2003, **27**, 1207–1215.
79 L. García-Río and J. R. Leis, *Chem. Commun.*, 2000, 455.
80 C. Cabaleiro-Lago, L. Garcia-Rio, P. Herves and J. Perez-Juste, *J. Phys. Chem. B*, 2005, **109**, 22614–22622.